Am. J. Hum. Genet. 64:446–461, 1999

De Novo *Alu*-Element Insertions in *FGFR2* Identify a Distinct Pathological Basis for Apert Syndrome

Michael Oldridge,[1] Elaine H. Zackai,[4] Donna M. McDonald-McGinn,[4] Sachiko Iseki,[2] Gillian M. Morriss-Kay,[2] Stephen R. F. Twigg,[1] David Johnson,[1] Steven A. Wall,[3] Wen Jiang,[5] Christiane Theda,[5] Ethylin Wang Jabs,[5] and Andrew O. M. Wilkie[1,3]

[1]Institute of Molecular Medicine, John Radcliffe Hospital, Oxford; [2]Department of Human Anatomy and Genetics, University of Oxford; [3]Oxford Craniofacial Unit, The Radcliffe Infirmary NHS Trust, Oxford; [4]Clinical Genetics Center, Children's Hospital of Philadelphia, Philadelphia; and [5]Departments of Pediatrics, Medicine and Surgery, The Johns Hopkins University School of Medicine, Baltimore

Summary

Apert syndrome, one of five craniosynostosis syndromes caused by allelic mutations of fibroblast growth-factor receptor 2 (FGFR2), is characterized by symmetrical bony syndactyly of the hands and feet. We have analyzed 260 unrelated patients, all but 2 of whom have missense mutations in exon 7, which affect a dipeptide in the linker region between the second and third immunoglobulin-like domains. Hence, the molecular mechanism of Apert syndrome is exquisitely specific. *FGFR2* mutations in the remaining two patients are distinct in position and nature. Surprisingly, each patient harbors an *Alu*-element insertion of ~360 bp, in one case just upstream of exon 9 and in the other case within exon 9 itself. The insertions are likely to be pathological, because they have arisen de novo; in both cases this occurred on the paternal chromosome. FGFR2 is present in alternatively spliced isoforms characterized by either the IIIb (exon 8) or IIIc (exon 9) domains (keratinocyte growth-factor receptor [KGFR] and bacterially expressed kinase, respectively), which are differentially expressed in mouse limbs on embryonic day 13. Splicing of exon 9 was examined in RNA extracted from fibroblasts and keratinocytes from one patient with an *Alu* insertion and two patients with Pfeiffer syndrome who had nucleotide substitutions of the exon 9 acceptor splice site. Ectopic expression of KGFR in the fibroblast lines correlated with the severity of limb abnormalities. This provides the first genetic evidence that signaling through KGFR causes syndactyly in Apert syndrome.

Received August 7, 1998; accepted for publication November 23, 1998; electronically published January 22, 1999.

Address for correspondence and reprints: Dr. A. O. M. Wilkie, Institute of Molecular Medicine, John Radcliffe Hospital, Headington, Oxford OX3 9DS, United Kingdom. E-mail: awilkie@worf.molbiol.ox.ac.uk

© 1999 by The American Journal of Human Genetics. All rights reserved.
0002-9297/99/6402-0029$02.00

Introduction

Apert syndrome (MIM 101200) is a severe autosomal dominant disorder characterized by craniosynostosis (premature fusion of the cranial sutures) and bilateral bony syndactyly of the hands and feet. A variety of other malformations occur at a lower frequency, including abnormalities of the skin, skeleton, brain, and other internal organs (Upton and Zuker 1991; Park et al. 1995; Slaney et al. 1996). It is one of five craniosynostosis syndromes associated with allelic mutations of the fibroblast growth-factor receptor (FGFR) 2 gene (*FGFR2*), along with Crouzon, Pfeiffer, Jackson-Weiss and Beare-Stevenson syndromes (reviewed in Wilkie 1997). Crouzon syndrome is characterized by apparently normal limbs, whereas in Pfeiffer syndrome (MIM 101600) the thumbs and halluces are broad and there is sometimes cutaneous syndactyly; the limb phenotype of Jackson-Weiss syndrome is variable and usually intermediate in severity (Gorlin et al. 1990); Beare-Stevenson syndrome is associated with the cutaneous disorders cutis gyrata and acanthosis nigricans (Przylepa et al. 1996).

FGFRs are transmembrane receptor tyrosine kinase proteins involved in signaling pathways via interaction with fibroblast growth factors (FGFs), 18 of which have been characterized to date (Hu et al. 1998; Ohbayashi et al. 1998). The receptors consist of three extracellular immunoglobulin-like domains (IgI, IgII, and IgIII), a transmembrane domain, and an intracellular split tyrosine kinase domain. After ligand binding, the receptors dimerize and signaling is activated by autophosphorylation of intracellular tyrosine residues (Spivak-Kroizman et al. 1994). The complexity of FGFR2 is increased by mutually exclusive alternative splicing of exons 8 and 9, leading to two forms of the receptor, keratinocyte growth-factor receptor (KGFR) and bacterially expressed kinase (BEK), which differ in the C-terminal half of the IgIII domain (exon numbering herein is based on the mouse *Fgfr2* described by Twigg et al. [1998]). KGFR is characterized by splicing of the IIIa (exon 7)

domain to the IIIb (exon 8) domain, whereas BEK is characterized by splicing of the IIIa domain to the IIIc (exon 9) domain (fig. 1). KGFR is expressed primarily in epithelial cell types, whereas BEK is expressed in other cell types, and the two isoforms have different ligand specificities: FGF7 and FGF10 bind specifically to KGFR, whereas BEK exhibits a broader ligand specificity (Dell and Williams 1992; Miki et al. 1992; Gilbert et al. 1993; Ornitz et al. 1996; Del Gatto et al. 1997; Carstens et al. 1998; Xu et al. 1998).

All FGFR2 mutations identified to date are dominantly inherited, and the observation that different craniosynostosis syndromes result from allelic missense mutations of the same gene implies that the mutations act by a variety of gain-of-function mechanisms. Within FGFR2, three main classes of mutation have been identified. Most patients in the Crouzon/Pfeiffer/Jackson-Weiss group have mutations clustered in the body of the third immunoglobulin-like domain, either in exon 7 (IIIa) or in exon 9 (IIIc) (fig. 1). The similar phenotype arising from mutation of these two exons argues that craniosynostosis is caused by abnormality of the BEK isoform, because the KGFR isoform is not affected by the exon 9 mutations. The mutations frequently involve gain or loss of cysteine or substitution of conserved buried residues, suggesting that they lead, directly or indirectly, to covalent dimerization of FGFR2 molecules and constitutive activation of signaling. Recent functional studies for certain mutations support the involvement of these mechanisms (Neilson and Friesel 1996; Robertson et al. 1998). The Beare-Stevenson mutations, substitutions to cysteine in the extracellular juxtamembrane region, constitute a distinct class but probably act by a similar mechanism.

The third class of mutations are those causing Apert syndrome, which show different properties and probably act by a distinct mechanism. They occur within the putative linker region between the IgII and IgIII domains, which is located in a sequence of 16 amino acids conserved between all four human FGFRs (Johnson and Williams 1993). Mutations of this region in FGFRl, FGFR2, and FGFR3 give rise to distinct syndromes. In FGFR2, we have identified, in 258/260 unrelated cases of Apert syndrome, mutations that involve amino acid substitutions of a serine-proline dipeptide in exon 7 (172 Ser252Trp, 1 Ser252Phe, and 85 Pro253Arg) (Park et al. 1995; Wilkie et al. 1995; Oldridge et al. 1997; and combined data of Oxford and Johns Hopkins groups [authors' unpublished data]). Equivalent Pro→Arg mutations in FGFR1 (Pro252Arg) and FGFR3 (Pro250Arg) cause Pfeiffer and Muenke syndromes, respectively (Muenke et al. 1994; Bellus et al. 1996). None of these mutations involves gain or loss of cysteine residues, but all are substitutions to bulky side-chain amino acids. Both the IgII and IgIII domains are involved in the binding of FGF ligand, suggesting that these mutations lead to changes in the relative orientation of the two domains and hence could accentuate ligand binding. Supporting

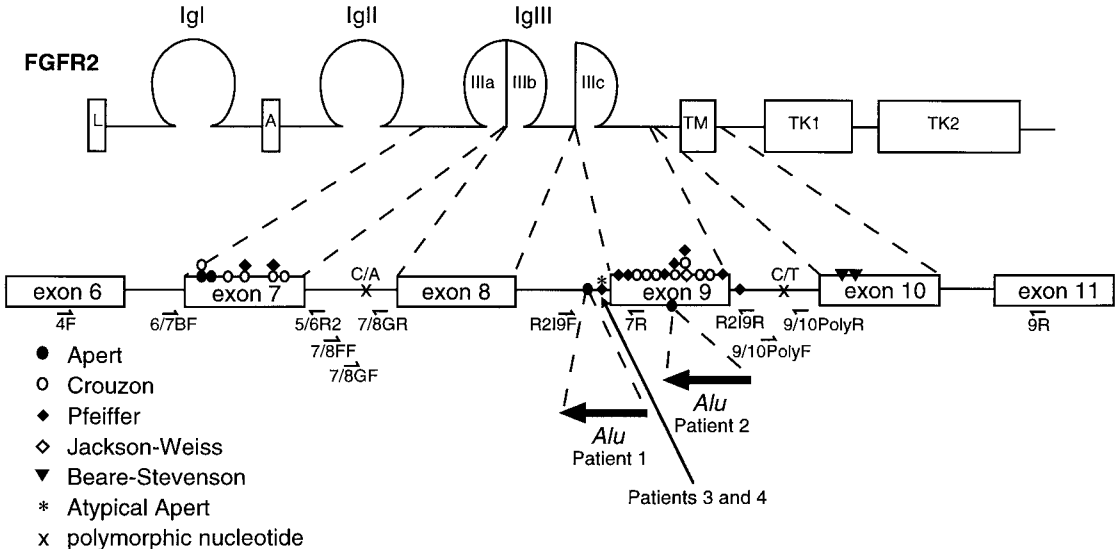

Figure 1 Structure of *FGFR2,* showing positions of mutations, polymorphic nucleotides, and primers used in the present study. The outline of FGFR2 protein (*top*) shows the leader sequence (L), acid box (A), three immunoglobulin-like domains (IgI, IgII, and IgIII), a transmembrane domain (TM), and a split tyrosine-kinase domain (TK1 and TK2). Alternative splicing of the second half of the IgIII domain is shown by IgIIIb (KGFR isoform) and IgIIIc (BEK isoform), encoded by exons and 8 and 9 respectively. Selected previously described mutations and the positions of the *Alu* insertions in patients 1 and 2 (with Apert syndrome), as well as the nucleotide substitution in patients 3 and 4 (with Pfeiffer syndrome), are shown diagrammatically on the partial genomic structure, along with the positions of primers (not to scale).

this is the recent demonstration that the Apert mutations cause reduced dissociation of FGF2 ligand from the BEK isoform of FGFR2, the effect being more marked for Ser252Trp than for Pro253Arg (Anderson et al. 1998*a*).

Although these recent findings provide insight into the molecular mechanism of the morphological abnormalities of Apert syndrome, they do not explain two other clinical observations. First, the two common mutations are associated with differential effects on cleft palate and syndactyly: cleft palate is more frequent with the Ser252Trp mutation, whereas syndactyly is more severe with the Pro253Arg mutation (Slaney et al. 1996). The latter trend runs counter to the prediction, from in vitro studies of BEK, that the Ser252Trp mutation should exhibit a greater biological effect (Anderson et al. 1998*a*). In one patient with a Ser252Trp mutation, the syndactyly was so mild that the phenotype suggested Pfeiffer syndrome rather than Apert syndrome (Passos-Bueno et al. 1998). Second, given the specificity of the Apert mutations, the report of a patient with a phenotype similar to Apert syndrome (craniosynostosis, 3-4 syndactyly of the hands, and complete syndactyly of the feet) but with a different molecular pathology was surprising (Passos-Bueno et al. 1997). This patient had a nucleotide substitution of the 3′ splice site upstream of exon 9, 1119-2A→G (cDNA numbering is from Dionne et al. 1990), a mutation elsewhere described in four cases of Pfeiffer syndrome (fig. 1) (Lajeunie et al. 1995; Schell et al. 1995; Passos-Bueno et al. 1997). These observations indicate that the mechanism of the syndactyly in Apert syndrome remains to be elucidated.

Here we describe the mutations identified in the 2 individuals, from our series of 260 patients with Apert syndrome, who did not have mutations of the exon 7 serine-proline dipeptide. Surprisingly, different de novo *Alu*-element insertions are present in both individuals: in one case the insertion lies just upstream of exon 9, and in the other case it is within the exon itself. Given the likely effects of these mutations on alternative splicing, we obtained fibroblast and keratinocyte cell lines from one of these patients, as well as from two patients with Pfeiffer syndrome who have point mutations at the position identical to that reported for the patient with atypical Apert syndrome reported by Passos-Bueno et al. (1997). The finding of ectopic KGFR expression in fibroblasts from these patients defines a new pathological class of FGFR2 mutations and leads us to formulate a hypothesis for the mechanism of syndactyly in Apert syndrome. This correlates with the expression pattern of the *Fgfr* isoforms in early mouse limb buds.

Subjects and Methods

Patients

Patient 1 is shown in figure 2*A*. She was born at 38 wk gestation, weighing 3.26 kg. At the time of her birth, her mother was age 35.1 years and was noted to have mild exorbitism; the father was age 35.4 years and was clinically normal. The patient had cranial features of Apert syndrome, with brachycephaly, hypertelorism, ocular proptosis, and midface hypoplasia. In addition, the palate was high arched but not cleft. Skull x-rays confirmed bicoronal synostosis. The hands and feet showed complete syndactyly of digits 1–5, corresponding to morphological scores of 3 (the most severe grade) (Upton 1991). On plain radiography (fig. 2*A*), the hands showed partial transverse fusion of the 4th and 5th metacarpals and longitudinal fusion of the proximal and middle phalanges of digits 3 and 4, and the thumbs had a single phalanx. The feet showed partial transverse fusion of the 1st and 2d metatarsals on the left and longitudinal fusion of the proximal and middle phalanges of digits 2–5. The halluces had a single large delta-shaped phalanx.

An unusual finding for Apert syndrome was scoliosis, noted at age 3 years. Radiographs of the spine showed multiple fusions of thoracic vertebrae T4–T9, with anomalous vertebral bodies and secondary rib fusions. Developmental progress was good, and the patient was attending a normal school at age 7 years. Surgery had been performed for her craniosynostosis, syndactyly, and scoliosis.

Patient 2 is shown in figure 2*B*. He had typical clinical features of Apert syndrome, as described elsewhere (case FA-17 reported by Park et al. [1995]). In brief, this male patient was born at 40 wk gestation, weighing 4.11 kg. The parents were clinically normal; at the time of the patient's birth, the mother was age 32.1 years, and the father was age 32.6 years. The patient's craniofacial anomalies included turribrachycephaly with craniosynostosis, hypertelorism, ocular proptosis, mild malar hypoplasia, choanal atresia, and a high, narrow, but noncleft palate. Scoliosis was diagnosed at age 1.5 years but has remained stable with physical therapy. On recent assessment at age 8.7 years, the patient's height was 123 cm (10th centile), and he had required surgery for craniosynostosis, syndactyly, and choanal atresia. There was complete syndactyly of the hands and feet (type 3). Severe developmental delay was apparent: he had no speech, communicated with simple signs, walked with a broad-based gait, and had poor fine-motor skills. Additional features were strabismus with amblyopia and bilateral contractures of the elbows with rhizomelia.

Patients 3 and 4 had Pfeiffer syndrome. Craniofacial features included exorbitism, ocular hypertelorism, and midface hypoplasia, and skull radiographs demonstrated craniosynostosis in both cases (not illustrated). These patients had limb phenotypes at the severe end of the spectrum for Pfeiffer syndrome, with very broad, radially deviated thumbs and halluces. In addition, patient 3 had 2-3 cutaneous syndactyly of the feet, and patient

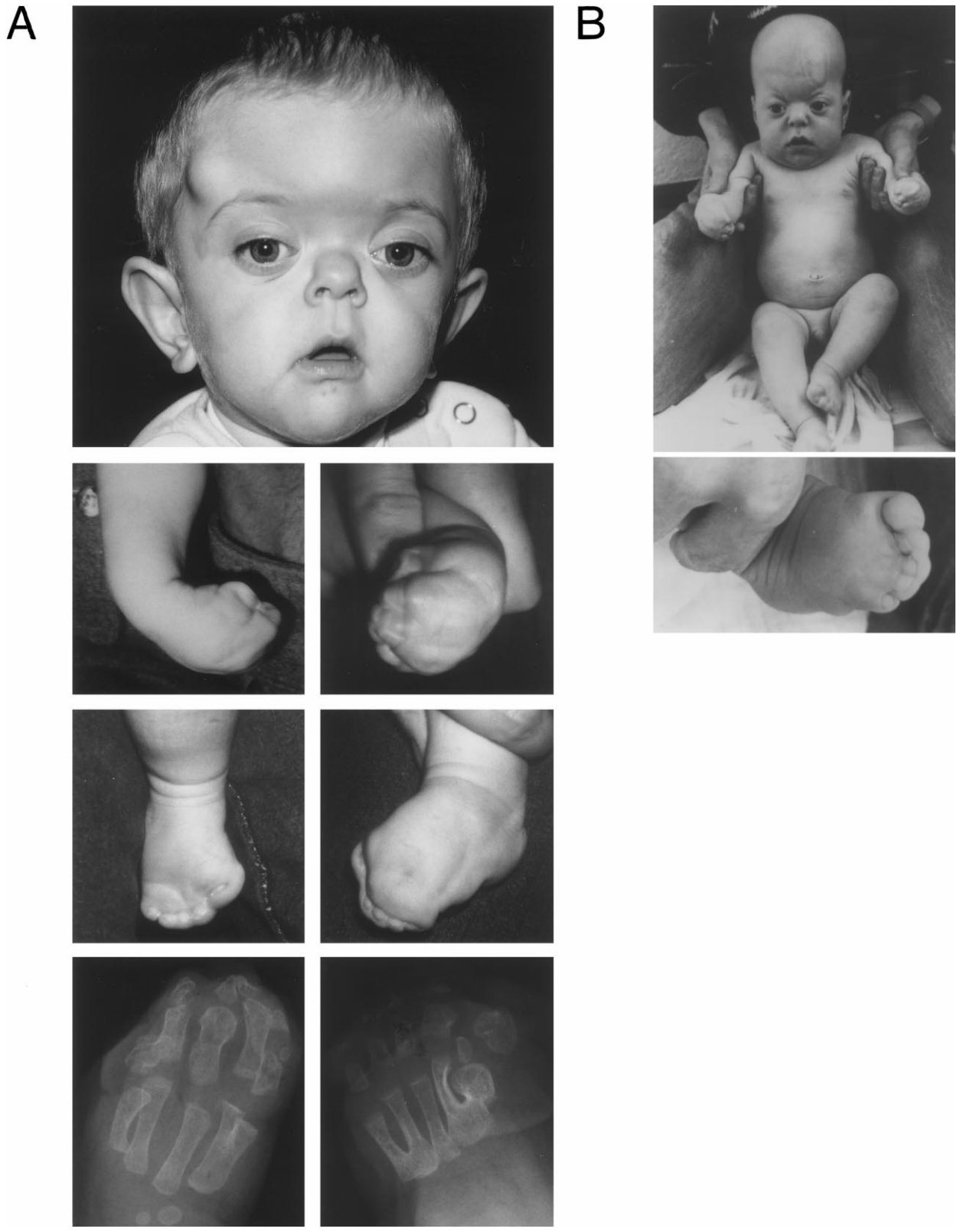

Figure 2 Phenotype of patients with Apert syndrome caused by *Alu*-element insertions. *A*, Patient 1, showing facial features post craniectomy and cranial remodeling (*top*), preoperative appearance of hands and feet (*middle*), and radiographs of right hand and left foot at age 5 mo (*bottom*). *B*, Patient 2, showing appearance of skull and limbs (*top*) and close-up of right foot (*bottom*).

4 had partial 1-2 cutaneous syndactyly of the feet (fig. 3). Radiographs of the hands and feet of patient 3 showed short, malformed 1st metacarpals and metatarsals. Mutations of *FGFR2* were identified in these patients by abnormal migration of exon 9 PCR products on single-strand conformational polymorphism gels, followed by direct sequencing (not illustrated). Patient 3 had a 1119-2A→G substitution of the 3′ splice site upstream of exon 9. This is a relatively common *FGFR2* mutation in Pfeiffer syndrome (Lajeunie et al. 1995; Schell et al. 1995; Passos-Bueno et al. 1997) and is identical to the mutation in the patient with atypical Apert syndrome described by Passos-Bueno et al. (1997). Patient 4 had a different substitution of the same nucleotide, 1119-2A→T, elsewhere described in a single patient with Pfeiffer syndrome (Anderson et al. 1998*b*).

For all sampling procedures, informed consent was given by the patients. Genomic DNA was prepared from peripheral blood samples. Skin biopsies were obtained, under general anesthetic, from patients 1, 3, and 4 during planned operative procedures and were used to obtain cultures of keratinocyte and fibroblast cells.

PCR Amplification

Oligonucleotides specific for *FGFR2* are listed in table 1, and their positions are indicated in figure 1. Généthon markers were purchased from Research Genetics. PCR was performed in a total volume of 25 μl containing 40 ng of DNA, 120 μM each dNTP, 10 mM Tris pH 9, 50 mM KCl, 1.5 mM $MgCl_2$, 0.1% Triton X-100, 0.01% gelatin, 0.4 μM primers, and 0.4 U of Ampli*Taq* DNA polymerase (Perkin-Elmer). Thermocycling was performed on a Hybaid Omnigene Temperature Cycler and, unless otherwise stated, consisted of one cycle of 4 min at 94°C, 1 min at 62°C, and 30 s at 72°C, followed by 33 cycles of 1 min at 94°C, 1 min at 62°C, and 30 s at

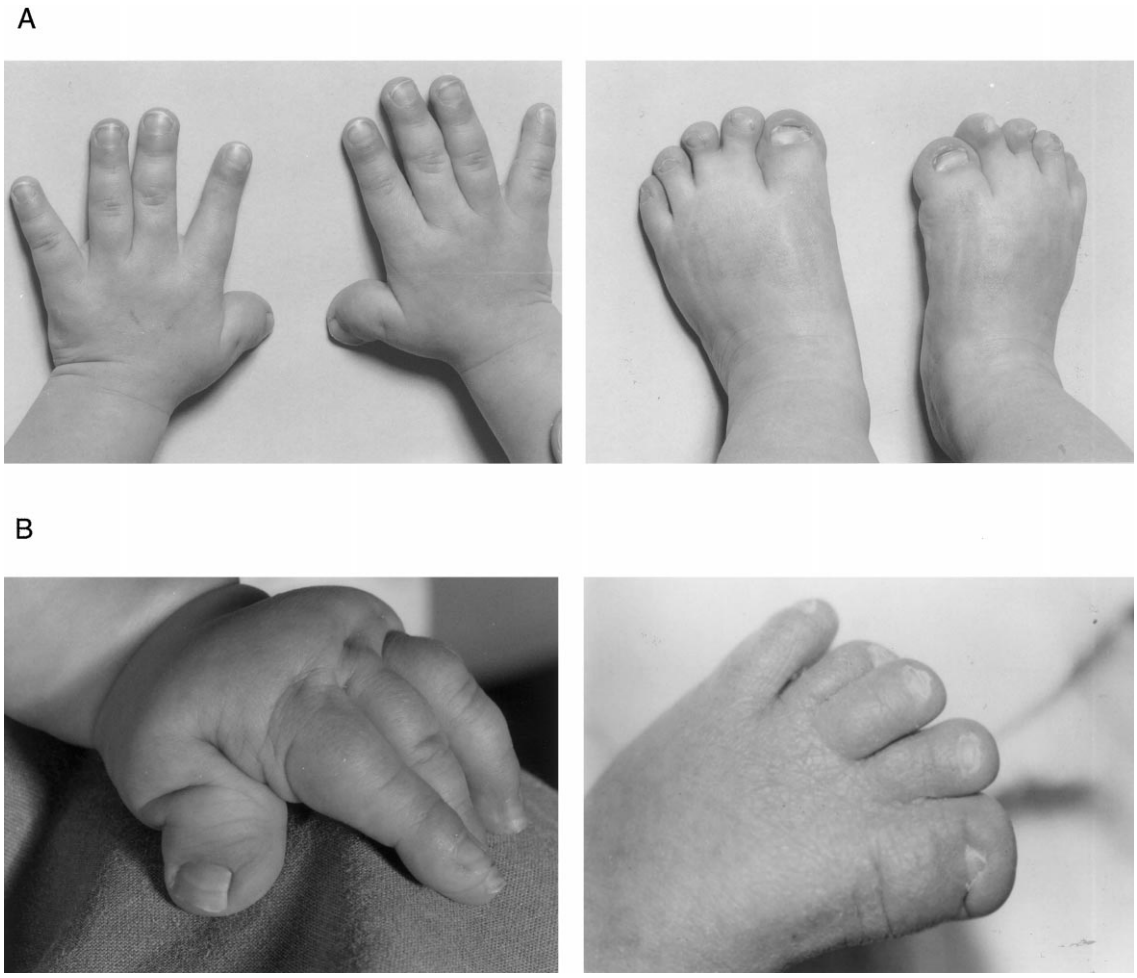

Figure 3 Appearance of limbs in patients with Pfeiffer syndrome who were investigated in the present study. *A*, Hands and feet of patient 3. *B*, Left hand and foot of patient 4.

Table 1

Sequence and Purpose of Oligonucleotides

Oligonucleotide	Sequence[a] (5′→3′)	Purpose
6/7BF	TGGCATGAGGTCACTGACAG	Exon 7 sequencing
5/6R2	CCAACAGGAAATCAAAGAACC	Exon 7 sequencing
R2I9F	AATCATTCCTGTGTCGTCTAACC	PCR across exon 9
R2I9R	AAAAACCCAGAGAGAAAGAACAG	PCR across exon 9
7/8GF	AAAACCCTGACCTTTGAAATCC	PCR of intron 7 polymorphism
7/8GR	CGTGGTAGGCAAGGAGTTAAGAG	PCR of intron 7 polymorphism
9/10PolyF	TGCTTTCATCCCACTTTG	PCR of intron 9 polymorphism
9/10PolyR	AGCAAACCACAGTCTCTG	PCR of intron 9 polymorphism
7/8FF	ATACTCTGTCCCCCATAGGGCGG	PCR of intron 7/*Alu* (patient 1)
7R	CAATCTCTTTGTCCGTGGTG	PCR of intron 7/*Alu* (patient 1)
DPOLC	GTCATATTTCTGCACCAGTG	Intron 7 ASO (C allele)
DPOLA	CACTGGTGCATAAATATGAC	Intron 7 ASO (A allele)
9/10PolyC	TAGAATGGACTTTCGGTT	Intron 9 ASO (C allele)
9/10PolyT	AACCAAAAGTCCATTCTA	Intron 9 ASO (T allele)
4F	GGGTCCATCAATCACACGTAC	RT-PCR
9R	GGCGTGTTGTTATCCTCACCAG	RT-PCR
SPL7/8	GTTCTCAAGCACTCGGGGA	Exon 7/8 junction oligonucleotide
SPL7/9	GTTCTCAAGGCCGCCGGT	Exon 7/9 junction oligonucleotide
SPL7/10	GTTCTCAAGCGCCTGGAAG	exon 7/10 junction oligonucleotide
SPL7/11	GTTCTCAAGGTTTCGGCTGA	Exon 7/11 junction oligonucleotide

[a] Polymorphic bases are underlined.

72°C and a final step of 1 min at 94°C, 1 min at 62°C, and 10 min at 72°C.

FGFR2 *Mutation Analysis*

DNA was prepared from leukocytes by proteinase K digestion and phenol/chloroform extraction. DNA was amplified by PCR using primers 6/7BF-5/6R2 (exon 7) and R2I9F-R2I9R (exon 9). The samples were run on 2% agarose gels, the bands were excised, and DNA was extracted by the Qiaquick gel-purification kit (Qiagen). The DNA was then sequenced with the primers cited above, by the Thermo Sequenase cycle-sequencing kit (Amersham).

Determination of Parental Origin of Alu *Insertions*

The patients and family members were genotyped for two polymorphisms within *FGFR2:* a C/A variant in intron 7 (Moloney et al. 1996) and a C/T variant in intron 9 (W. Jiang, unpublished data). Genotypes at the C/A variant were determined by *Bsg*I digestion of the 7/8GF-7/8GR PCR product (Moloney et al. 1996). Genotypes at the C/T variant were determined by electrophoresis of duplicate 9/10PolyF-9/10PolyR PCR products on 2% agarose gels, blotting onto Zeta probe membrane (Bio-Rad), and hybridization with allele-specific oligonucleotides (ASOs) for the T and C alleles—9/10PolyT and 9/10PolyC, respectively. The hybridization was performed at 42°C in 7% polyethylene glycol/10% SDS, and washing performed at 65°C in 2 × SSC/0.1% SDS for 10 min. Correct paternity of offspring was confirmed by use of the polymorphic CA-repeat markers *D1S207, D2S102, D6S470, D16S407,* and *D20S27* (Dib et al. 1996).

DNA was amplified by PCR using primers flanking both an informative polymorphism and the site of *Alu* insertion, by the Expand kit (Boehringer Mannheim). In patient 1, the C/A variant was amplified with the primer pair 7/8FF-7R, with an extension time of 3 min. In patient 2, the C/T variant was amplified with primer pair R2I9F-9/10PolyR, with an extension time of 2 min. The products were run in duplicate on 1% agarose gels and hybridized with oligonucleotides designed to bind to one or the other of the polymorphic alleles. Hybridization and washing were performed as described above.

RNA Analysis

RNA was prepared from fibroblast and keratinocyte cell lines derived from skin samples (Chomczynski and Sacchi 1987). Reverse transcriptase–PCR (RT-PCR) was performed with 10 μg of RNA in first-strand synthesis in a total of 40 μl containing 340 pmol of random hexamer primers, 32 U of RNase inhibitor (Boehringer Mannheim), and 400 U of Moloney murine leukemia virus reverse transcriptase (Gibco BRL). Four microliters of cDNA was then used in a PCR reaction containing 40 μM dNTP with the primer pair 4F-9R, to amplify the segment of the *FGFR2* message starting in exon 6 and finishing in exon 11 (1-min extension time). The products were run on a 2% agarose gel, blotted, and hybridized to oligonucleotides designed to bind specifi-

cally to various splice variants (table 1). The conditions for hybridization were as described above. To measure the *BEK*:*KGFR* ratio, 50 pmol of primer 4F was 5′ end-labeled with T4 polynucleotide kinase (New England Biolabs) in a volume of 25 μl and was purified by being passed through a Sephadex G25 column. One microliter of labeled primer was used with 0.4 μM unlabeled 4F and 9R and 4 μl of cDNA, in a PCR reaction with 28 amplification cycles (pilot experiments established that this was prior to the plateau phase). The products were digested with either *Hpa*I (which cleaves *BEK* but not *KGFR*) or *Ava*I (which cleaves *KGFR* but not *BEK*), and the samples were run on a nondenaturing polyacrylamide gel (8% acrylamide [w/v], 0.27% bisacrylamide, 1 × Tris-borate EDTA) at 35 V for 6 h. The gel was exposed to a Storage Phosphor Screen (Kodak) overnight, and the radioactivity was quantified on a Storm 850 PhosphorImager (Molecular Dynamics). The relative intensities of the digested and undigested products were analyzed by Storm Imagequant software.

In Situ Hybridization of Embryonic Mouse Limbs

In situ hybridization was performed on paraformaldehyde-fixed whole limbs from mouse embryos obtained 13 d after mating (E13), with digoxygenin-labeled riboprobes specific for the mouse *Fgfr2* splice variants *Bek* and *Kgfr*. For the *Bek*-specific probe, a 162-bp *Ppu*MI-*Hae*II fragment from the mouse *Bek* cDNA IgIIIc region was used as template. For the *Kgfr*-specific probe, a 122-bp *Ppu*MI-*Eco*RV fragment from the mouse *Kgfr* cDNA IgIIIb region was used. Antisense and sense transcripts were generated as described elsewhere (Iseki et al. 1997). The specimens were subsequently embedded in gloop (a mixture of glutaraldehyde and albumen), for vibratome sectioning at 50 μm, to detect tissue-specific localization of RNA transcripts.

Results

Identification of Alu*-Element Insertions in Patients 1 and 2*

The DNA sequence of exon 7 was normal. We analyzed exon 9 for mutations, by amplification with oligonucleotides R2I9F and R2I9R, which correspond to sequences in the flanking introns. Surprisingly, fragments of ~590 bp and ~575 bp were generated from the DNA of patients 1 and 2, respectively, in addition to the expected product of 225 bp; the larger fragments were not present in unaffected relatives (fig. 4*A* and *B*). The larger PCR fragments were excised, gel purified, and sequenced. Both were found to contain *Alu*-element insertions. Patient 1 has an insertion of 368 bp within intron 8, 1119-3–-4ins*Alu*. The *Alu* element is inserted in the orientation opposite to that of *FGFR2* and contains a run of 69 A residues at its 3′ end and a repeat flanking sequence of 16 bp (fig. 4*C*). Patient 2 has an insertion of ~350 bp (the exact number of A residues was not determined) within exon 9, 1220–1221 ins*Alu*. This *Alu* element is also inserted in the opposite orientation and contains a run of 44–50 A residues with a repeat flanking sequence of 15 bp (fig. 4*D*). The sequence of the flanking direct repeats does not match the proposed consensus very closely, although the pentanucleotide 5′ TAGAA-3′ (relative to the *Alu* sense strand) is shared by both insertions at one of the proposed sites of nicking (Jurka 1997). In figure 5, the sequence of the two *Alu* elements inserted is compared with that of *Alu* Y–family members described elsewhere (Batzer et al. 1996) and with previously identified disease-causing *Alu* elements (table 2). The *Alu* element in patient 1 is most closely related to the *Alu*Ya5 family, whereas the *Alu* element in patient 2 is most closely related to the *Alu*Yb8 family.

Both *Alu* insertions arose de novo in the patients. In family 1 this was demonstrated directly (fig. 4*A*), whereas in family 2, in the absence of a DNA sample from the deceased father, this could be deduced because sibling A21 inherited the same *FGFR2* haplotype from the father (not illustrated) but did not show the insertion (fig. 4*B*).

Parental Origin of Alu *Insertions*

Family 1 was informative for a C/A polymorphism in intron 7 (patient 1, CA; mother, CC; father, AA). The DNA segment containing both the polymorphism and the *Alu* insertion was amplified with primers 7/8FF and 7R: in addition to the normal ~2.25-kb band, the patient showed a ~2.60-kb band containing the *Alu* element (fig. 6*A*). Duplicate gels were blotted and hybridized to ASOs. Oligonucleotide DPOLC hybridized to the maternal fragment and to the patient's normal-sized fragment, whereas oligonucleotide DPOLA hybridized to the paternal fragment and to the patient's larger *Alu*-containing fragment, demonstrating the paternal origin of the *Alu* (fig. 6*A*).

Patient 2 was homozygous for the intron 7 polymorphism but heterozygous for the C/T polymorphism in intron 9. Although the mother was also heterozygous for the intron 9 polymorphism, by creating haplotypes we deduced that patient 2 had received the T allele from his mother and had received the C allele from his father (not illustrated). Amplification with primers R2I9F and 9/10PolyR yielded a product containing the informative polymorphism and the *Alu* insertion. Duplicate gels were blotted and hybridized to ASOs. 9/10PolyT hybridized to the normal allele of the patient, and 9/10PolyC hybridized to the allele containing the *Alu* insertion (fig.

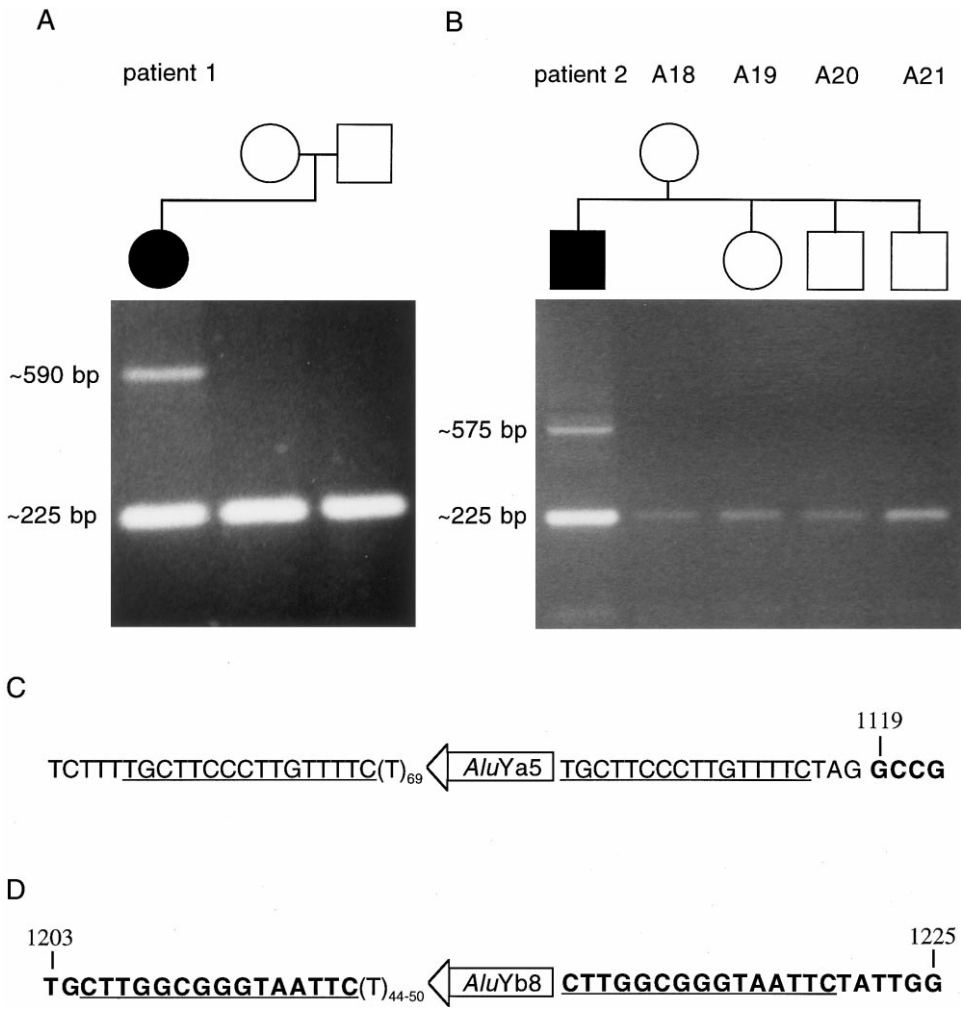

Figure 4 Amplification of *FGFR2* exon 9 and flanking intron sequence. *A* and *B*, PCR products from patients 1 (*A*) and 2 (*B*) and their available family members, with primers R2I9F and R2I9R. All samples contained the expected 225-bp product, but patients 1 and 2 also showed DNA fragments of ~590 bp and ~575 bp, respectively, containing the inserted *Alu* elements. *C*, Position and orientation of *Alu* element inserted into intron 8 of patient 1. *D*, Position and orientation of *Alu* element inserted into exon 9 of patient 2. The repeat flanking sequence is underlined, the exon sequence is boldface, and cDNA is based on the numbering used by Dionne et al. (1990).

6*B*). This showed that the *Alu* insertion is in *cis* to the C allele and therefore is also paternally derived.

We conclude that both mutations probably arose in the father's germ line, in keeping with the exclusively paternal origin of new mutations in Apert syndrome that has been described elsewhere (Moloney et al. 1996). Integration into the paternally derived chromosome during early embryogenesis is a possibility, although there was no evidence of mosaicism in either patient.

Analysis of FGFR2 *Splicing*

The position of the *Alu* element in patient 1, just upstream of the start of exon 9, suggested that it might affect utilization of the 3′ splice site, leading to the generation of different splice forms. Mutations of this acceptor site have been recorded in several cases of Pfeiffer syndrome and in one patient with an Apert-like phenotype (see Introduction), although the consequences for splicing have not previously been investigated. We considered it important to document the effect of splicing in these cases and studied two patients with Pfeiffer syndrome: patient 3, with a 1119-2A→G mutation, and patient 4, with a 1119-2A→T mutation (these mutations are henceforth referred to as "-2A→G" and "-2A→T," respectively). Of note is that both these patients had very marked radial deviation and broadening of the 1st digits of both the hands and feet, with some soft-tissue syndactyly (fig. 3*A* and *B*).

We prepared cDNA from fibroblasts and keratinocytes derived from representative controls, patients with

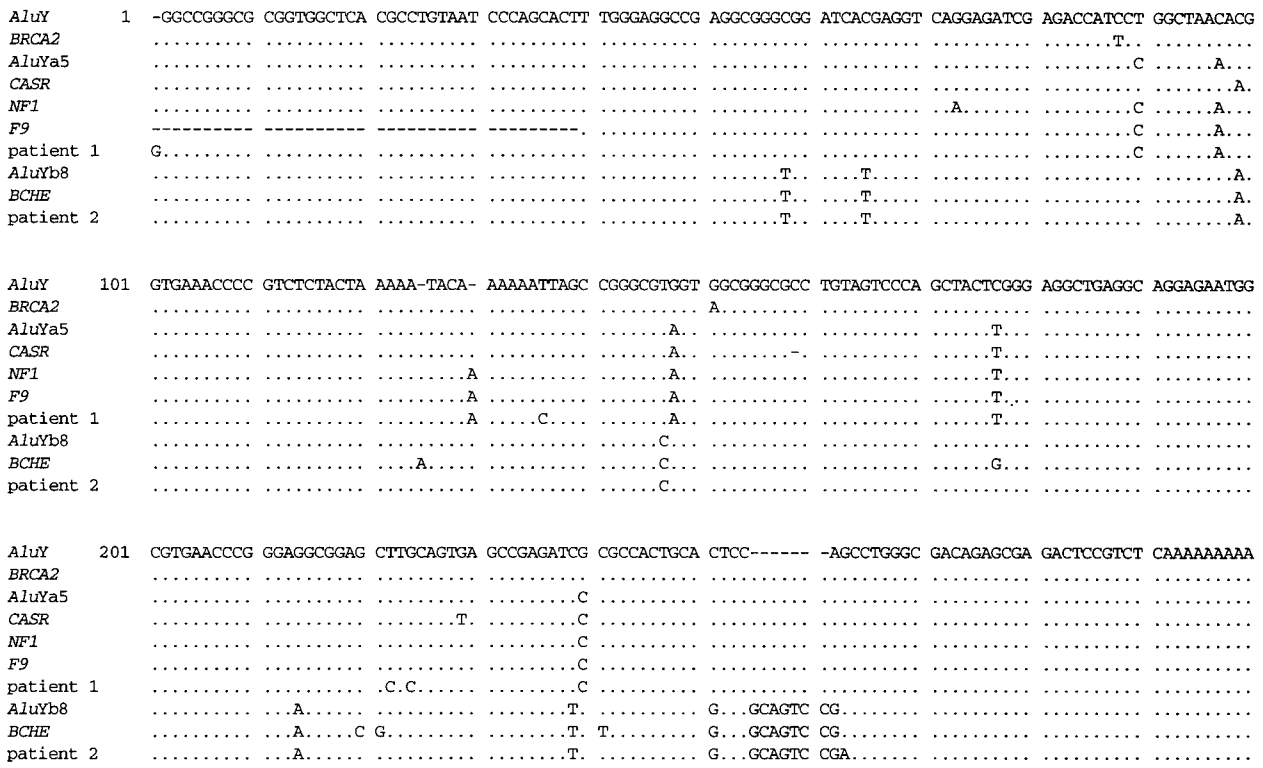

Figure 5 Sequence of *Alu* elements inserted into patients 1 and 2, compared with *Alu* Y family members (Batzer et al. 1996) and previously described pathological *Alu* insertions (table 2). *Alu* Y = major *Alu* subfamily; *BRCA2* = breast cancer gene; *Alu* Ya5 = *Alu* Y subfamily member; *CASR* = calcium-sensing receptor gene; *NF1* = neurofibromin gene; *F9* = factor IX gene; *Alu* Yb8 = *Alu* Y subfamily member; *BCHE* = cholinesterase gene.

the canonical Apert syndrome mutations, patient 1 (with the *Alu* insertion), and patients 3 and 4 (with Pfeiffer syndrome) (these cell lines were not available from patient 2). RT-PCR was performed with primers located within exons 6 (4F) and 11 (9R), encompassing the entire IgIII and transmembrane domains, to avoid biased amplification of particular alternatively spliced products (fig. 1). A single major RT-PCR product of ~640 bp was obtained from all samples, which corresponds in size to the full-length KGFR (exons 6-7-8-10-11) or BEK (exons 6-7-9-10-11) isoforms. In addition, a number of faint lower-molecular-weight bands were visible in some lanes (fig. 7, *top panel*).

To identify the splice forms corresponding to the PCR products, we blotted the gel and hybridized the products with oligonucleotides specific to various exon junction fragments. The results of hybridization to SPL7/9 (specific for the BEK isoform) and SPL7/8 (specific for the KGFR isoform) are shown in figure 7. Whereas, as expected, fibroblast lines from a normal individual and patients with canonical Apert mutations expressed only BEK, the fibroblasts from patients 1, 3, and 4 demonstrated ectopic KGFR expression (fig. 7, *middle and bottom panels*). All the keratinocyte cell lines showed only KGFR expression. Additional, fainter RT-PCR products in figure 7, most apparent in the fibroblast lines of patients 1, 3, and 4, were identified as 6-7-10-11 and 6-7-11 splice forms, by oligonucleotides SPL7/10 and SPL7/11, respectively. We conclude that mutations of the *3′* splice site of exon 9 indeed disrupt normal utilization of this exon in fibroblasts. The ectopic expression of KGFR is particularly interesting, because this would extend the ligand sensitivity of the cell to include FGF7 and FGF10.

To determine whether the limb-phenotype differences between patients 1, 3, and 4 correlated with the level of ectopic KGFR expression, we performed preliminary quantitation experiments by measuring the relative amounts of the two isoforms after restriction-enzyme cleavage (see Subjects and Methods). Patient 1, with the *Alu* insertion causing Apert syndrome, showed the highest ectopic expression of KGFR, with 23% of the total expression of KGFR and BEK, followed by patient 3, with 12%, and patient 4, with 4%. If these values are normalized to an equal level of BEK expression (which assumes that all BEK is expressed from the wild-type

Table 2

Comparison of Pathological *Alu* Insertions

Gene	Disorder	*Alu* Family	Insertion	Orientation	De Novo?	Functional Effect	Reference
NF1	Neurofibromatosis	Ya5	Intron	Antisense	Yes	Exon skipping→ truncation	Wallace et al. (1991)
BCHE	Acholinesterasemia	Yb8	Exon	Sense	No		Muratani et al. (1991)
F9	Hemophilia B	Ya5	Exon	Sense	Yes		Vidaud et al. (1993)
CASR	Familial hypocalciuric hypercalcemia	Ya5	Exon	Antisense	No		Janicic et al. (1995)
BRCA2	Breast cancer	Y	Exon	Sense		Exon skipping→ truncation	Miki et al. (1996)
APC	Hereditary desmoid disease		Exon	Sense	No		Halling et al. (1997)
BTK	X-linked agammaglobulinemia	Y	Exon	Antisense	Yes		Lester et al. (1997)
IL2RG	X-linked severe combined immunodeficiency	Ya5	Intron	Antisense	No		Lester et al. (1997)
EYA1	Branchio-oto-renal syndrome	Ya5	Exon	Antisense	Yes		Abdelhak et al. (1997)
FGFR2	Apert syndrome	Ya5	Intron	Antisense	Yes	Ectopic expression of alternative splice form	Present study
FGFR2	Apert syndrome	Yb8	Exon	Antisense	Yes		Present study

allele and that the BEK expression level is equal in the three patients), the ratio of ectopic KGFR expression in patients 1, 3, and 4 is approximately 7:3:1.

Expression of Kgfr *and* Bek *Isoforms in Embryonic Mouse Limbs*

In whole E13 mouse limbs, both *Kgfr*- and *Bek*-specific probes hybridized to the interdigital mesenchyme, with the *Bek*-specific probe giving a signal much more intense than that of *Kgfr* (fig. 8*A* and *B*). *Bek* expression was also detectable both adjacent to the differentiated cartilage and at the growing tips of the digits (fig. 8*B*). Sections revealed that both *Fgfr2* isoforms were expressed in the surface ectoderm, but *Kgfr* transcripts were more abundant than *Bek* transcripts (fig. 8C and *D*). The sections also confirmed that, in the interdigital mesenchyme, *Bek* transcripts were more abundant than *Kgfr* transcripts; similarly, both probes hybridized to the mesenchyme surrounding the digital cartilages, but *Bek* gave a much stronger signal. Overall, these results indicate that, although both splice variants of *Fgfr2* are expressed in both mesenchymal and epithelial tissues in the early hand plate, *Kgfr* expression predominates in the surface epithelium whereas *Bek* is predominantly mesenchymal.

Discussion

We have studied 260 patients with Apert syndrome and have found that all but 2 have mutations of a Ser-Pro dipeptide in the linker region between the IgII and IgIII domains of FGFR2 (exon 7). The 2 patients described in the present paper have a phenotype very similar to that in the other 258 cases, including craniosynostosis and severe syndactyly of the hands and feet, but harbor very different mutations; both contain *Alu*-element insertions, the first just upstream of exon 9 and the second within the middle of exon 9.

The finding of independent, de novo *Alu* insertions in *FGFR2,* separated by only 105 bp, in the two patients with Apert syndrome who have a normal sequence of the Ser-Pro dipeptide is strong evidence that these insertions cause the Apert phenotype in these patients. The observation that a very similar, specific phenotype may result from two distinct mutational processes affecting different parts of *FGFR2* is remarkable, and no explanation of the phenotypic similarity is immediately obvious. However, this may be viewed as an opportunity to seek a deeper understanding of the mechanism(s) by which Apert mutations lead to the characteristic morphological abnormalities. Before considering this, however, we will first discuss a distinct area of biology il-

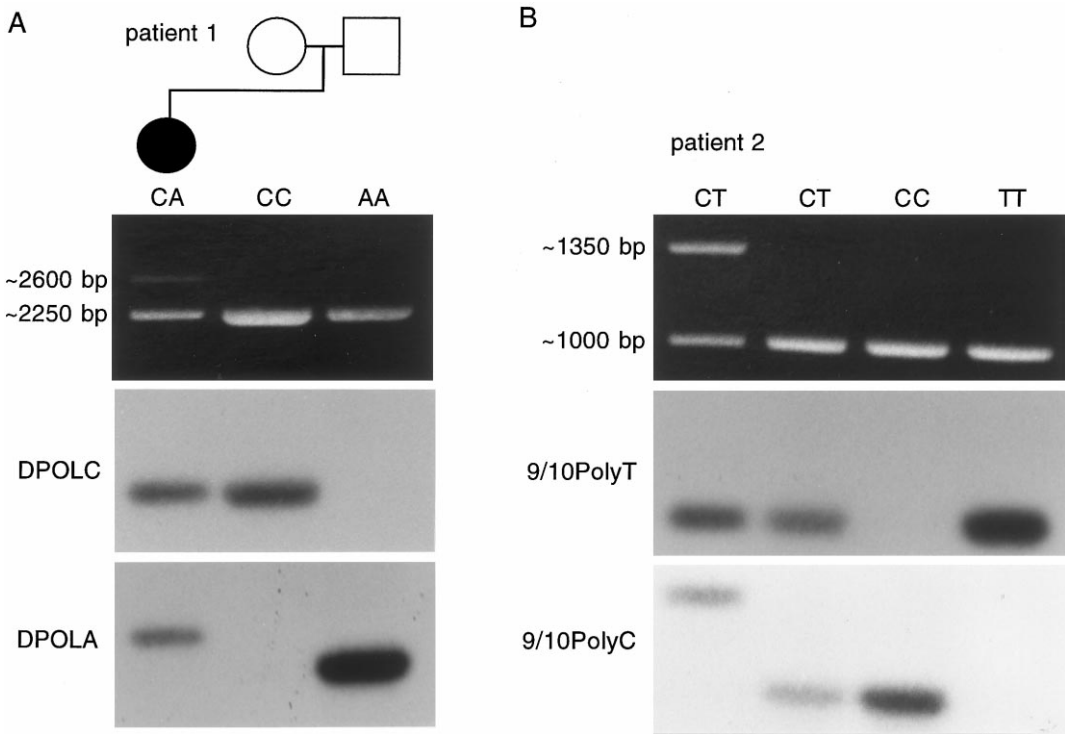

Figure 6 Paternal origin of *Alu* insertions. *A,* Patient 1 and parents, analyzed for intron 7 (C/A) polymorphism. *Top,* PCR-amplification products, with primers 7/8FF and 7R. *Bottom,* Results of hybridization to oligonucleotides DPOLC and DPOLA, specific for the C and A alleles, respectively. The *Alu*-containing allele originates from the father. *B,* Patient 2 and controls, analyzed for intron 9 (C/T) polymorphism. *Top,* PCR-amplification products, with primers R2I9F and 9/10PolyR. *Bottom,* Results of hybridization to oligonucleotides 9/10PolyT and 9/10PolyC, specific for the T and C alleles, respectively. The *Alu*-containing allele hybridizes to the C-specific oligonucleotide, indicating that it is paternally derived.

luminated by this work, the process of *Alu*-element retroposition.

Biology of Alu *Insertion*

The *Alu* elements are members of the short interspersed nuclear element (SINE) family of repeat elements and are the most abundant complex repeats found within the human genome, at a copy number of >500,000 (reviewed by Schmid 1996). They are evolutionarily derived from the 7SL RNA gene, and their mobilization is thought to arise from transcription by RNA polymerase III, followed by coupled reverse transcription/integration into the genome. The poly-A tract is indicative of an RNA intermediate, and the flanking repeats provide a signature for the mechanism of integration. Retroposition of *Alu* elements is believed to require L1 reverse transcriptase, although the precise mechanism remains unproved (Boeke 1997).

The major phase of *Alu* expansion is thought to have occurred 40 million years ago, and it is estimated that, at present, de novo *Alu*-integration events occur rarely, ~1/100 births (Deininger and Batzer 1995). Relatively recent *Alu* integrations may manifest as phenotypically silent polymorphisms in the human population (Batzer et al. 1995) or as pathological mutations: table 2 summarizes both the nine pathological *Alu* insertions that have been described elsewhere and the two cases presented here. The *Alu* sequences can be divided into different subfamilies, according to diagnostic mutations of the consensus sequence. The *Alu* insertions in patients 1 and 2 are most closely related to the Ya5 and Yb8 subfamilies, respectively, with the major diagnostic difference between the two being the insertion of a 7-bp sequence in the Yb8 subfamily (fig. 5). Both, however, are distinct from previously described mutations. Both Ya5 and Yb8 are subsets of the *Alu*Y subfamily. This youngest of the major subfamilies represents only 0.4% of genomic *Alu* elements, but all pathological *Alu* insertions (including those from patients 1 and 2) belong to this subfamily, indicating that only a small number of source *Alu* genes are actively mobile.

Comparison, in table 2, of the pathological *Alu* insertions described elsewhere and the two *FGFR2* insertions described here highlights the following points. First, all mutations described elsewhere have affected different genes, whereas we have identified two inde-

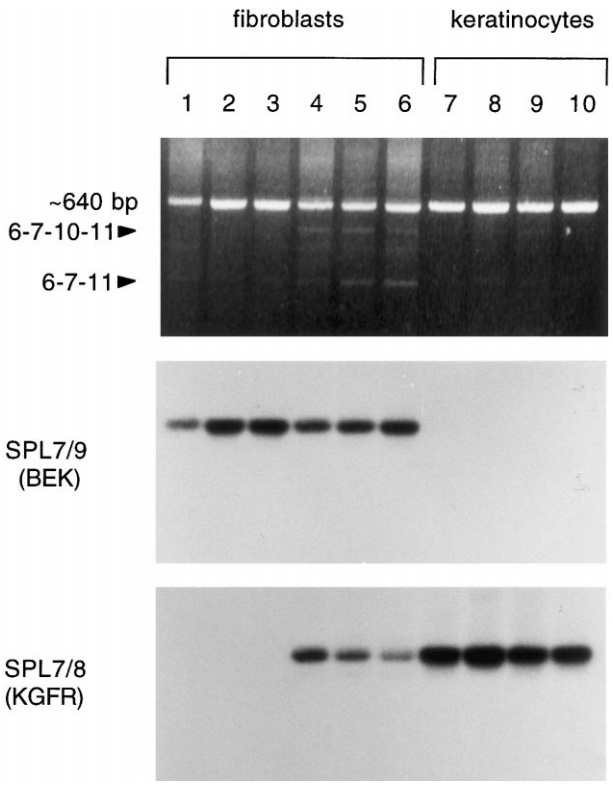

Figure 7 Analysis of FGFR2 expression in fibroblasts and keratinocytes from patients with FGFR2 mutations. *Top,* PCR-amplification products from cDNA, by primers 4F (exon 6) and 9R (exon 11). Lanes 1–6, Products from fibroblast cell lines: lane 1, normal control; lane 2, Apert (Ser252Trp); lane 3, Apert (Pro253Arg); lane 4, patient 1; lane 5, patient 3; lane 6, patient 4. Lanes 7–10, Products from keratinocyte cell lines: lane 7, Crouzon (Gly338Arg); lane 8, Apert (Ser252Trp); lane 9, patient l; lane 10, patient 4. Arrowheads indicate minor products identified by their size and hybridization to the specific splice-junction oligonucleotides, SPL7/10 and SPL7/11. *Bottom,* Results of hybridization to oligonucleotides SPL7/9 and SPL7/8, which are specific to the BEK and KGFR isoforms, respectively.

pendent *Alu* insertions into *FGFR2,* only 105 bp apart. Second, all the disorders in which *Alu* insertions have elsewhere been described either are recessive or are dominant haploinsufficiencies, indicating loss of function; by contrast, Apert syndrome is considered to be a dominant, gain-of-function disorder. Third, in the only two cases analyzed elsewhere at the RNA level (*NF1* and *BRCA2*), the *Alu* insertion was shown to cause exon skipping, setting a precedent for the alteration of *FGFR2* splicing that we have observed. Evidence that the *Alu* insertions act by a novel gain-of-function mechanism is discussed below.

Pathogenesis of Syndactyly in Apert Syndrome: Insights from Alu *Insertions*

The discovery of *Alu* insertions within or just upstream of the alternatively spliced exon 9 (IIIc) is surprising, because many missense mutations of this exon have elsewhere been described in craniosynostosis syndromes (Crouzon, Pfeiffer, and Jackson-Weiss syndromes) with normal or mild limb phenotypes (fig. 1). An explanation of the Apert phenotype of the *Alu* mutations must account for this discrepancy. Our hypothesis that the insertions might disrupt the normal splicing of the IIIc exon would also have to explain why previously described mutations of the 3′ splice site of exon 9 usually had been found to result in a Pfeiffer syndrome phenotype, although in a single instance an Apert-like phenotype had been observed (Lajeunie et al. 1995; Schell et al. 1995; Passos-Bueno et al. 1997). We therefore chose to include in our study two patients with Pfeiffer syndrome who had mutations of this splice site. Of note is that the limb abnormalities of these patients (fig. 3) were more severe than those in any of the other patients with Pfeiffer syndrome in our series, with very broad, medially deviated first digits of both hands and feet and with some soft-tissue syndactyly. Corroborating this, a recent study of the feet of 22 patients with Pfeiffer syndrome identified the most severe abnormalities in a patient with the same *FGFR2* mutation as was seen in our patient 4 (Anderson et al. 1998*b*).

Analysis of *FGFR2* expression in keratinocyte and fibroblast lines from patient 1, with Apert syndrome and the *Alu* insertion, and from the patients with Pfeiffer syndrome revealed ectopic expression of the KGFR isoform within fibroblasts, which was not observed in fibroblasts from patients with either of the canonical Apert mutations. Our findings contrast with the situation in vitro, in which partial deletion of exon 9 did not lead to alternative use of exon 8 (Gilbert et al. 1993). The level of ectopic *KGFR* expression differed between cell lines, being highest in patient 1, with the *Alu* insertion, intermediate in patient 3, with Pfeiffer syndrome and the -2A→G mutation, and lowest in patient 4, with Pfeiffer syndrome and the -2A→T mutation. To assess the likely consequences that ectopic *KGFR* expression has for limb development, we examined expression of both the *Kgfr* and *Bek* isoforms in the embryonic mouse limb bud. At E13, *Kgfr* was expressed only at low levels in the interdigital or peridigital mesenchyme, whereas *Bek* was expressed at much higher levels (fig. 8). Although expression of *Fgfr2* isoforms in the early limb bud has not been examined in detail elsewhere, these findings conform with the general conclusions of previous studies (Orr-Urtreger et al. 1993; Finch et al. 1995). Therefore, ectopic expression of *Kgfr* in the mesenchyme should extend the ligand sensitivity of the mesenchymal cells, to include FGF7 and FGF10 (Ornitz et al. 1996; Xu et al. 1998). Previous studies confirm that FGF10 is present at significant levels in the limb-bud mesenchyme, whereas FGF7 expression occurs later, once myogenesis and chondrogenesis are established

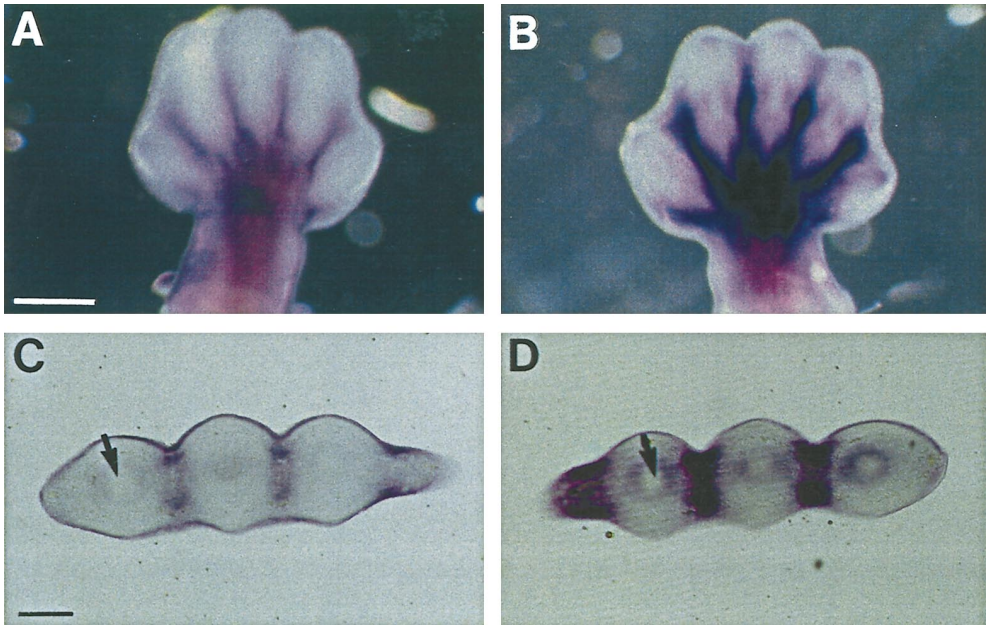

Figure 8 E13 mouse embryonic limb buds hybridized with probes specific for *Kgfr* (*A* and *C*) and *Bek* (*B* and *D*). In situ hybridization was performed on whole specimens (*A* and *B*), which were then sectioned (*C* and *D*). Both probes show hybridization to interdigital mesenchyme, but the level of *Bek* transcripts is much higher than that of *Kgfr; Bek* expression is also clearly detectable both around the digital cartilages (*arrow*) and at the growing digital tips (*B* and *D*). In the surface ectoderm, *Kgfr* expression is stronger than *Bek* expression (*C* and *D*). Scale bars represent 500 μm (in the case of *A* and *B*) and 20 μm (in the case of *C* and *D*).

(Mason et al. 1994; Finch et al. 1995; Ohuchi et al. 1997; reviewed by Martin 1998). By analogy with the effects of increased FGF-induced signaling in the cranial sutures (Iseki et al. 1997), this could favor skeletogenesis in the limb-bud mesenchyme, both around the digital cartilages and in the interdigital tissue, leading to syndactyly.

If we assume that the magnitude of ectopic expression observed in fibroblast lines from the patients reflects the in vivo situation, then signal activation would be greater for the patient with the *Alu* insertion than for the patients with Pfeiffer syndrome and would account for the greater severity of limb abnormalities in patients with Pfeiffer syndrome who have mutations of the exon 9 splice site compared with those who have other *FGFR2* mutations. It is of interest that fibroblasts from patient 3 (with Pfeiffer syndrome) with the -2A→G mutation showed higher ectopic *KGFR* expression than was seen in those from the patient with the -2A→T mutation. The patient with the Apert-like phenotype described by Passos-Bueno et al. (1997) had the -2A→G mutation, and we speculate that chance effects (perhaps of genetic background) led to abnormally high ectopic *KGFR* expression in this individual, exceeding the threshold required for syndactyly. Variability in ectopic KGFR expression might account for the diversity of limb phenotypes (ranging from normal to Apert-like) in craniosynostosis families such as that described by Escobar and Bixler (1977), although the mutation in that family has not been reported.

Conclusions

Our observation of a correlation between ectopic *KGFR* expression in fibroblasts and severity of syndactyly provides, to our knowledge, the first genetic evidence that the syndactyly of Apert syndrome is a KGFR-mediated effect, as speculated in the original report of *FGFR2* mutations in Apert syndrome (Wilkie et al. 1995). Our model assumes that the effects observed in fibroblasts reflect those in the early embryo. A report of ectopic *KGFR* expression in fibroblasts from a patient with syndromic acanthosis nigricans but not syndactyly suggests that additional factors may be important (Hughes et al. 1998). It should be noted that lower levels of additional splice variants (6-7-10-11 and 6-7-11) were observed. The 6-7-11 product has been described in FGFR2, by Katoh et al. (1992), and may represent a physiological splice variant (Johnston et al. 1995), whereas the 6-7-10-11 product is out of frame and probably pathological. It is unclear to what extent these additional splice variants may contribute to the phenotype. Unfortunately, we were unable to study cell lines from patient 2, in whom the *Alu* insertion occurred within

exon 9 itself. We propose that this mutation would also cause exon skipping, as has been described in the case of *BRCA2* (Miki et al. 1996). Clearly, we cannot formally exclude other possibilities, such as expression of the entire expanded exon or the activation of a cryptic splice site within the *Alu* sequence (Makalowski et al. 1994). Nevertheless, the phenotypic similarity resulting from the two *Alu* insertions argues that they act by a shared pathological mechanism.

Our model proposes, by extension from these observations, that the syndactyly associated with canonical Apert mutations (Ser252Trp and Pro253Arg) is also KGFR mediated. By analogy with the in vitro effect that the canonical Apert mutations have on the BEK isoform (Anderson et al. 1998*a*), we anticipate that the canonical mutations will cause reduced dissociation of ligand(s)—most likely FGF7 or FGF10—from the KGFR isoform. This would lead to enhanced KGFR-mediated signaling, as postulated for the *Alu* insertion mutations. Given the greater severity of syndactyly associated with the Pro253Arg mutation (Slaney et al. 1996), this mutation is expected to exhibit enhanced ligand affinity, compared with Ser252Trp. Our hypothesis that the syndactyly of Apert syndrome is KGFR mediated can be further tested both by studies of in vitro binding of FGF to mutant KGFR molecules and by analysis in animal models.

Acknowledgments

We are very grateful to all the families for their cooperation in this study; to D. M. Moloney for obtaining samples; to S. Walsh for genotyping of Apert mutations; to S. Butler, C. He, and M. Hughes for help with the cell culture; to P. L. Deininger, J. K. Heath, and M. R. Passos-Bueno for discussions; and to D. J. Weatherall for support. This work was funded by a Wellcome Trust Prize Studentship (to M.O.), Action Research (to G.M.M.-K.), National Institutes of Health grants R01 DE11441 and PCRU-GCRC RR00052 (to E.W.J.), and a Wellcome Trust Senior Research Fellowship in Clinical Science (to A.O.M.W.).

Electronic-Database Information

The accession number and URL for data in this article are as follows:

Online Mendelian Inheritance in Man (OMIM): http://www.ncbi.nlm.nih.gov/Omim (for Apert syndrome [MIM 101200] and Pfeiffer syndrome [MIM 101600])

References

Abdelhak S, Kalatzis V, Heilig R, Compain S, Samson D, Vincent C, Levi-Acobas F, et al (1997) Clustering of mutations responsible for branchio-oto-renal (BOR) syndrome in the *eyes absent* homologous region (eyaHR) of *EYA1*. Hum Mol Genet 6:2247–2255

Anderson J, Burns HD, Enriquez-Harris P, Wilkie AOM, Heath JK (1998a) Apert syndrome mutations in fibroblast growth factor receptor 2 exhibit increased affinity for FGF ligand. Hum Mol Genet 7:1475–1483

Anderson PJ, Hall CM, Evans RD, Jones BM, Hayward RD (1998b) The feet in Pfeiffer's syndrome. J Craniofac Surg 9: 83–87

Batzer MA, Deininger PL, Hellmann-Blumberg U, Jurka J, Labuda D, Rubin CM, Schmid CW, et al (1996) Standardized nomenclature for Alu repeats. J Mol Evol 42:3–6

Batzer MA, Rubin CM, Hellmann-Blumberg U, Alegria-Hartman M, Leeflang EP, Stern JD, Bazan HA, et al (1995) Dispersion and insertion polymorphism in two small subfamilies of recently amplified human *Alu* repeats. J Mol Biol 247:418–427

Bellus GA, Gaudenz K, Zackai EH, Clark LA, Szabo J, Francomano CA, Muenke M (1996) Identical mutations in three different fibroblast growth factor receptor genes in autosomal dominant craniosynostosis syndromes. Nat Genet 14: 174–176

Boeke JD (1997) LINEs and *Alus* - the polyA connection. Nat Genet 16:6–7

Carstens RP, McKeehan WL, Garcia-Blanco MA (1998) An intronic sequence element mediates both activation and repression of rat fibroblast growth factor receptor 2 pre-mRNA splicing. Mol Cell Biol 18:2205–2217

Chomczynski P, Sacchi N (1987) Single-step method of RNA isolation by acid guanidinium thiocyanate-phenol-chloroform extraction. Anal Biochem 162:156–159

Deininger PL, Batzer MA (1995) SINE master genes and population biology. In: Maraia R (ed) The impact of short, interspersed elements (SINES) on the host genome. RG Landes, Georgetown, TX, pp 43–60

Del Gatto F, Plet A, Gesnel M-C, Fort C, Breathnach R (1997) Multiple interdependent sequence elements control splicing of a fibroblast growth factor receptor 2 alternative exon. Mol Cell Biol 17:5106–5116

Dell KR, Williams LT (1992) A novel form of fibroblast growth factor receptor 2: alternative splicing of the third immunoglobulin like domain confers ligand binding specificity. J Biol Chem 267:21225–21229

Dib C, Fauré S, Fizames C, Samson D, Drouot N, Vignal A, Millasseau P, et al (1996) A comprehensive genetic map of the human genome based on 5,264 microsatellites. Nature 380:152–154

Dionne CA, Crumley G, Bellot F, Kaplow JM, Searfoss G, Ruta M, Burgess WH, et al (1990) Cloning and expression of two distinct high-affinity receptors cross-reacting with acidic and basic fibroblast growth factors. EMBO J 9:2685–2692

Escobar V, Bixler D (1977) On the classification of the acrocephalosyndactyly syndromes. Clin Genet 12:169–178

Finch PW, Cunha GR, Rubin JS, Wong J, Ron D (1995) Pattern of keratinocyte growth factor and keratinocyte growth factor receptor expression during mouse fetal development suggests a role in mediating morphogenetic mesenchymal-epithelial interactions. Dev Dyn 203:223–240

Gilbert E, Del Gatto F, Champion-Arnaud P, Gesnel M-C, Breathnach R (1993) Control of BEK and K-SAM splice sites

in alternative splicing of the fibroblast growth factor receptor 2 pre-mRNA. Mol Cell Biol 13:5461–5468

Gorlin RJ, Cohen MM Jr, Levin LS (1990) Syndromes with craniosynostosis: general aspects and well-known syndromes. In: Gorlin RJ, Cohen MM Jr, Levin LS (eds) Syndromes of the head and neck, 2d ed. Oxford University Press, New York, pp 519–539

Halling KC, Honchel R, Lazzaro CR, Bufill JA, Arndt C, Lindor NM (1997) A germline *AluI* repeat insertion of the APC gene leading to hereditary desmoid disease in an Amish family. Am J Hum Genet Suppl 61:A67

Hu MC-T, Qiu WR, Wang Y-P, Hill D, Ring BD, Scully S, Bolon B, et al (1998) FGF-18, a novel member of the fibroblast growth factor family, stimulates hepatic and intestinal proliferation. Mol Cell Biol 18:6063–6074

Hughes AE, Armstrong DKB, Dawson JF, Nevin NC (1998) Syndromic acanthosis nigricans—evidence of aberrant fibroblast growth factor receptor function. Am J Hum Genet Suppl 63:A183

Iseki S, Wilkie AOM, Heath JK, Ishimaru T, Eto K, Morriss-Kay GM (1997) *Fgfr2* and *osteopontin* domains in the developing skull vault are mutually exclusive and can be altered by locally applied FGF2. Development 124: 3375–3384

Janicic N, Pausova Z, Cole DEC, Hendy GN (1995) Insertion of an Alu sequence in the Ca^{2+}-sensing receptor gene in familial hypocalciuric hypercalcemia and neonatal severe hyperparathyroidism. Am J Hum Genet 56:880–886

Johnson DE, Williams LT (1993) Structural and functional diversity in the FGF receptor multigene family. In: Vande Woude GF, Klein G (eds) Advances in cancer research. Vol 60. Academic Press, San Diego, pp 1–41

Johnston CL, Cox HC, Gomm JJ, Coombes RC (1995) Fibroblast growth factor receptors (FGFRs) localize in different cellular compartments. J Biol Chem 270:30643–30650

Jurka J (1997) Sequence patterns indicate an enzymatic involvement in integration of mammalian retroposons. Proc Natl Acad Sci USA 94:1872–1877

Katoh M, Hattori Y, Sasaki H, Tanaka M, Sugano K, Yazaki Y, Sugimura T, et al (1992) K-*sam* gene encodes secreted as well as transmembrane receptor tyrosine kinase. Proc Natl Acad Sci USA 89:2960–2964

Lajeunie E, Ma HW, Bonaventure J, Munnich A, Le Merrer M, Renier D (1995) *FGFR2* mutations in Pfeiffer syndrome. Nat Genet 9:108

Lester T, McMahon C, Van Regemorter N, Jones A, Genet S (1997) X-linked immunodeficiency caused by insertion of Alu repeat sequences. J Med Genet 34 Suppl 1:S81

Makalowski W, Mitchell GA, Labuda D (1994) Alu sequences in the coding regions of mRNA: a source of protein variability. Trends Genet 10:188–193

Martin GR (1998) The roles of FGFs in the early development of vertebrate limbs. Genes Dev 12:1571–1586

Mason IJ, Fuller-Pace F, Smith R, Dickson C (1994) FGF7 (keratinocyte growth factor) expression during mouse development suggests roles in myogenesis, forebrain regionalisation and epithelial-mesenchymal interactions. Mech Dev 45:15–30

Miki T, Bottaro DP, Fleming TP, Smith CL, Burgess WH, Chan AM-L, Aaronson SA (1992) Determination of ligand-binding specificity by alternative splicing: two distinct growth factor receptors encoded by a single gene. Proc Natl Acad Sci USA 89:246–250

Miki Y, Katagiri T, Kasumi F, Yoshimoto T, Nakamura Y (1996) Mutation analysis in the *BRCA2* gene in primary breast cancers. Nat Genet 13:245–247

Moloney DM, Slaney SF, Oldridge M, Wall SA, Sahlin P, Stenman G, Wilkie AOM (1996) Exclusive paternal origin of new mutations in Apert syndrome. Nat Genet 13:48–53

Muenke M, Schell U, Hehr A, Robin NH, Losken HW, Schinzel A, Pulleyn LJ, et al (1994) A common mutation in the fibroblast growth factor receptor 1 gene in Pfeiffer syndrome. Nat Genet 8:269–274

Muratani K, Hada T, Yamamoto Y, Kaneko T, Shigeto Y, Ohue T, Furuyama J, et al (1991) Inactivation of the cholinesterase gene by *Alu* insertion: possible mechanism for human gene transposition. Proc Natl Acad Sci USA 88:11315–11319

Neilson KM, Friesel R (1996) Ligand-independent activation of fibroblast growth factor receptors by point mutations in the extracellular, transmembrane, and kinase domains. J Biol Chem 271:25049–25057

Ohbayashi N, Hoshikawa M, Kimura S, Yamasaki M, Fukui S, Itoh N (1998) Structure and expression of the mRNA encoding a novel fibroblast growth factor, FGF-18. J Biol Chem 273:18161–18164

Ohuchi H, Nakagawa T, Yamamoto A, Araga A, Ohata T, Ishimaru Y, Yoshioka H, et al (1997) The mesenchymal factor, FGF10, initiates and maintains the outgrowth of the chick limb bud through interaction with FGF8, an apical ectodermal factor. Development 124:2235–2244

Oldridge M, Lunt PW, Zackai EH, McDonald-McGinn DM, Muenke M, Moloney DM, Twigg SRF, et al (1997) Genotype-phenotype correlation for nucleotide substitutions in the IgII- IgIII linker of *FGFR2*. Hum Mol Genet 6:137–143

Ornitz DM, Xu J, Colvin JS, McEwen DG, MacArthur CA, Coulier F, Gao G, et al (1996) Receptor specificity of the fibroblast growth factor family. J Biol Chem 271: 15292–15297

Orr-Urtreger A, Bedford MT, Burakova T, Arman E, Zimmer Y, Yayon A, Givol D, et al (1993) Developmental localization of the splicing alternatives of fibroblast growth factor receptor-2 (FGFR2). Dev Biol 158:475–486

Park W-J, Theda C, Maestri NE, Meyers GA, Fryburg JS, Dufresne C, Cohen MM Jr, et al (1995) Analysis of phenotypic features and FGFR2 mutations in Apert syndrome. Am J Hum Genet 57:321–328

Passos-Bueno MR, Richieri-Costa A, Sertié AL, Kneppers A (1998) Presence of the Apert canonical S252W FGFR2 mutation in a patient without severe syndactyly. J Med Genet 35:677–679

Passos-Bueno MR, Sertié AL, Zatz M, Richieri-Costa A (1997) Pfeiffer mutation in an Apert patient: how wide is the spectrum of variability due to mutations in the FGFR2 gene? Am J Med Genet 71:243–245

Przylepa KA, Paznekas W, Zhang M, Golabi M, Bias W, Bamshad MJ, Carey JC, et al (1996) Fibroblast growth factor receptor 2 mutations in Beare-Stevenson cutis gyrata syndrome. Nat Genet 13:492–494

Robertson SC, Meyer AN, Hart KC, Galvin BD, Webster MK, Donoghue DJ (1998) Activating mutations in the extracel-

lular domain of the fibroblast growth factor receptor 2 function by disruption of the disulfide bond in the third immunoglobulin-like domain. Proc Natl Acad Sci USA 95: 4567–4572

Schell U, Hehr A, Feldman GJ, Robin NH, Zackai EH, de Die-Smulders C, Viskochil DH, et al (1995) Mutations in *FGFR1* and *FGFR2* cause familial and sporadic Pfeiffer syndrome. Hum Mol Genet 4:323–328

Schmid CW (1996) Alu: structure, origin, evolution, significance, and function of one-tenth of human DNA. Prog Nucleic Acid Res Mol Biol 53:283–319

Slaney SF, Oldridge M, Hurst JA, Morriss-Kay GM, Hall CM, Poole MD, Wilkie AOM (1996) Differential effects of FGFR2 mutations on syndactyly and cleft palate in Apert syndrome. Am J Hum Genet 58:923–932

Spivak-Kroizman T, Lemmon MA, Dikic I, Ladbury JE, Pinchasi D, Huang J, Jaye M, et al (1994) Heparin-induced oligomerization of FGF molecules is responsible for FGF receptor dimerization, activation, and cell proliferation. Cell 79:1015–1024

Twigg SRF, Burns HD, Oldridge M, Heath JK, Wilkie AOM (1998) Conserved use of a non-canonical 5′ splice site (/GA) in alternative splicing by fibroblast growth factor receptors l, 2 and 3. Hum Mol Genet 7:685–691

Upton J (1991) Classification and pathologic anatomy of limb anomalies. Clin Plast Surg 18:321–355

Upton J, Zuker RM (eds) (1991) Clinics in plastic surgery. Vol 18: Apert syndrome. WB Saunders, Philadelphia

Vidaud D, Vidaud M, Bahnak BR, Siguret V, Sanchez SG, Laurian Y, Meyer D, et al (1993) Haemophilia B due to a de novo insertion of a human-specific *Alu* subfamily member within the coding region of the factor IX gene. Eur J Hum Genet 1:30–36

Wallace MR, Anderson LB, Saulino AM, Gregory PE, Glover TW, Collins FS (1991) A *de novo Alu* insertion results in neurofibromatosis type 1. Nature 353:864–866

Wilkie AOM (1997) Craniosynostosis: genes and mechanisms. Hum Mol Genet 6:1647–1656

Wilkie AOM, Slaney SF, Oldridge M, Poole MD, Ashworth GJ, Hockley AD, Hayward RD, et al (1995) Apert syndrome results from localized mutations of *FGFR2* and is allelic with Crouzon syndrome. Nat Genet 9:165–172

Xu X, Weinstein M, Li C, Naski M, Cohen RI, Ornitz DM, Leder P, et al (1998) Fibroblast growth factor receptor 2 (FGFR2)-mediated reciprocal regulation loop between FGF8 and FGF10 is essential for limb induction. Development 125:753–765